Translational Oncology 68 (2026) 102763

Contents lists available at ScienceDirect

Translational Oncology

journal homepage: www.elsevier.com/locate/tranon

STC2-mediated calcium homeostasis dysregulation in the osteosarcoma microenvironment: Insights from single-cell sequencing and machine learning

Kang Yao [a,b,1], Qian Jiawei [a,b,1], Xu Jietao [a,b], Wang Xijun [c,d,e], Zhou Hong [f], Bi Qing [g,h,i,*], Lv Jun [a,b,*]

[a] Cancer Center, Department of Orthopedics, Zhejiang Provincial People's Hospital, Affiliated People's Hospital, Hangzhou Medical College, Hangzhou, Zhejiang, China
[b] Department of Laboratory Medicine, Zhejiang Provincial People's Hospital, Affiliated People's Hospital, Hangzhou Medical College, Hangzhou, Zhejiang, China
[c] Department of Head and Neck Surgery, Sun Yat-sen University Cancer Center, Guangzhou, China
[d] State Key laboratory of Oncology in South China, Guangzhou, Guangdong, China
[e] Collaborative innovation Center for Cancer Medicine, Guangzhou, Guangdong, China
[f] Center for Plastic & Reconstructive Surgery, Department of Orthopedics, Zhejiang Provincial People's Hospital, Affiliated People's Hospital, Hangzhou Medical College, Hangzhou, Zhejiang, China
[g] Department of Sports Medicine, Zhejiang Provincial People's Hospital, Affiliated People's Hospital, Hangzhou Medical College, Hangzhou, Zhejiang, China
[h] Center for Rehabilitation Medicine, Department of Orthopedics, Zhejiang Provincial People's Hospital, Affiliated People's Hospital, Hangzhou Medical College, Hangzhou, Zhejiang, China
[i] Institute of Sports Medicine and Osteoarthropathy of Hangzhou Medical College, Hangzhou, Zhejiang, China

ARTICLE INFO

Keywords:
Osteosarcoma
Single-cell sequencing
Machine learning
Calcium homeostasis
STC2

ABSTRACT

Background: Osteosarcoma (OS) is an aggressive bone malignancy with a poor prognosis. Dysregulated calcium homeostasis may contribute to OS progression.

Methods: Various machine learning algorithms were integrated into multiple model combinations to identify key prognostic genes. Single-cell expression profiling was conducted to assess STC2 expression across different cell types within the OS microenvironment. Experimental validation was performed in OS cell lines (U2OS and 143B) using lentiviral shRNA-mediated knockdown, qPCR, proliferation assays, and migration/invasion assays. Immune infiltration and potential immunotherapy response were further explored using immune deconvolution, immune checkpoint analysis, TIDE, and SubMap.

Results: Calcium homeostasis-related dysregulation was associated with osteosarcoma progression, and machine-learning analysis identified STC2 as the most important prognostic gene. Single-cell analysis revealed that STC2 was predominantly expressed in endothelial, fibroblast, and malignant cells. In vitro experiments showed that knockdown of STC2 in OS cells significantly inhibited cell proliferation, migration, and invasion. Specifically, CCK-8, colony formation, and EdU assays demonstrated decreased cell proliferation, while Transwell assays revealed reduced migratory and invasive capacities of STC2-knockdown OS cells. Moreover, TIDE and SubMap analyses suggested that low STC2 expression was computationally associated with a higher predicted likelihood of response to immune checkpoint inhibitors.

Conclusions: Our findings suggest that calcium homeostasis dysregulation is involved in OS progression and that STC2 is a prioritized prognostic and functional candidate within this network. The findings suggest that STC2 may serve as a potential therapeutic target and candidate biomarker for OS, including in the context of predicted immunotherapy response, although this requires further validation.

* Corresponding authors at: Institute of Sports Medicine and Osteoarthropathy of Hangzhou Medical College, Hangzhou, Zhejiang, China.
E-mail addresses: bqzjsrmyy@163.com (B. Qing), 13858010120@163.com (L. Jun).
[1] Co-first authors

https://doi.org/10.1016/j.tranon.2026.102763
Received 2 February 2026; Received in revised form 16 March 2026; Accepted 9 April 2026

Introduction

Osteosarcoma (OS) is the most common primary malignant bone tumor in children and adolescents and is characterized by aggressive progression and an unfavorable prognosis, particularly in patients with metastasis or recurrence[1,2]. Despite advancements in surgical techniques and chemotherapy, the survival rate for patients with metastatic OS remains dismal, often below 30 % [3,4]. The underlying molecular mechanisms driving OS progression and metastasis remain incompletely understood, and this gap in knowledge significantly hinders the development of more effective treatment strategies [5]. Therefore, identifying biologically meaningful molecular programs involved in OS progression is of substantial clinical importance.

Calcium homeostasis plays a central role in multiple cellular processes, including proliferation, apoptosis, differentiation, and stress adaptation, many of which are dysregulated in cancer [6,7]. Alterations in calcium signaling pathways have been implicated in the initiation and progression of multiple cancers, including OS [8]. Disruptions in calcium ion regulation or the activity of calcium-binding proteins can influence tumor behavior, metastasis, and response to treatment [9,10]. However, the biological significance of calcium homeostasis-related dysregulation in OS remains insufficiently defined, particularly in relation to metastatic progression, prognostic stratification, and tumor microenvironmental heterogeneity. A systematic investigation of calcium homeostasis-related genes may therefore provide new insight into OS biology and reveal clinically relevant therapeutic candidates.

In recent years, machine learning (ML) has emerged as a transformative tool in cancer research, enabling the analysis of large-scale genomic and clinical data to identify biomarkers and predict patient outcomes with remarkable accuracy [11,12]. Compared with conventional single-gene approaches, ML-based frameworks are better suited to capture complex relationships among genes and to construct multigene prognostic models [13,14]. In this study, we apply a range of advanced ML techniques to analyze publicly available transcriptomic and clinical data from OS patients, with the goal of identifying key genes associated with calcium homeostasis that significantly impact patient survival. By integrating gene expression data with clinical outcomes, we aim to construct a robust prognostic model for OS, which could assist in stratifying patients and informing treatment decisions.

In this study, we integrated multiple ML algorithms to systematically investigate calcium homeostasis-related genes in OS using publicly available transcriptomic and clinical datasets. Our aim was to determine whether calcium homeostasis dysregulation is associated with OS progression and prognosis, and to identify prioritized candidate genes for downstream validation. Within this framework, STC2 emerged as the most robust prognostic candidate. We further explored its cellular distribution in the OS microenvironment, its association with immune-related features, and its biological effects in vitro. Together, this study provides a transcriptome-based framework linking calcium homeostasis-related dysregulation to OS progression and identifies STC2 as a key functional candidate that warrants further investigation.

Methods

Data acquisition and preprocessing

In this study, four publicly available OS datasets were utilized: Target-OS, GSE42352, GSE21257, and GSE39055. Among these, Target-OS, GSE21257, and GSE39055 provided comprehensive transcriptomic and survival data, which were employed for survival analysis and predictive modeling. The GSE42352 dataset, which includes normal tissue samples, was specifically used for differential expression analysis. Genes associated with calcium homeostasis (GO: BP_CALCIUM_ION_HOMEOSTASIS, $n = 329$) were obtained from The Molecular Signatures Database (MSigDB, https://www.gsea-msigdb.org/gsea/index.jsp). Prior to downstream analyses, all datasets underwent preprocessing and quality control. Samples with overall survival time shorter than 30 days were excluded to reduce potential bias caused by non-tumor-related early mortality. In addition, only samples with >10,000 detected genes were retained to ensure sufficient transcriptomic coverage and data quality for subsequent analyses. Missing clinical values were not imputed in the current study. After filtering, the datasets were normalized and prepared for subsequent integrative and cohort-specific analyses.

Batch effect removal and analysis of calcium homeostasis pathway in OS

To reduce batch effects between datasets, particularly between Target-OS and GSE42352, batch correction was performed using the ComBat algorithm [15,16]. The effectiveness of correction was assessed by density plots before and after correction. After correction, the activity of the calcium homeostasis pathway was quantified using single-sample Gene Set Enrichment Analysis (ssGSEA) based on the predefined calcium homeostasis-related gene set. Differential analysis was then performed to compare calcium homeostasis pathway scores between metastatic and non-metastatic OS samples, as well as between OS and normal control samples. To identify candidate prognostic genes, univariate Cox regression was used as an initial screening step, and genes with $p < 0.1$ were retained for downstream analysis. Gene-gene correlations were visualized using a heatmap, and protein-protein interaction (PPI) network analysis was performed to further explore the relationships among these genes.

Machine learning-based prognostic modeling of calcium homeostasis in OS

To construct a prognostic model for calcium homeostasis-related genes in OS, the Target-OS dataset was used as the training set, while GSE21257 and GSE39055 served as validation cohorts. The primary comparison in this study was performed among transcriptome-based machine-learning survival models. A total of 101 model combinations were generated by applying a range of machine learning algorithms, including regularization methods (such as LASSO and elastic net), tree-based methods (random survival forest (RSF) and generalized boosted regression model (GBM)), dimensionality reduction techniques (supervised principal components (SuperPC)), regression models for survival analysis (ridge regression, partial least squares regression for Cox (plsRcox), stepwise Cox regression), and support vector machine approaches (survival support vector machine (Survival-SVM)). The C-index was computed for each algorithm across all datasets to assess its predictive performance. The algorithms were then ranked by their average C-index, and the best-performing combination was selected for further refinement. Patients were stratified into high- and low-risk groups using the median riskScore as the cutoff. This cutoff was selected as a simple and reproducible distribution-based threshold that could be applied consistently across datasets without introducing additional outcome-driven optimization.

Analysis of immune pathways and biological mechanisms associated with risk score

To investigate the relationship between riskScore and immune-related pathways, we first identified 18 immune therapy-related pathways through a comprehensive literature search [17]. Additionally, Hallmark gene sets were retrieved from the MSigDB database for further analysis. Correlation analysis was performed to explore the associations between riskScore and these immune-related pathways. To better understand the biological mechanisms underlying risk stratification, Gene Ontology (GO) and Kyoto Encyclopedia of Genes and Genomes (KEGG) pathway analyses were conducted for both high- and low-risk groups.

Single-cell analysis of STC2 expression in OS

To explore the cellular expression of STC2 in OS at the single-cell

level, we used the TISCH2 database and analyzed the OS_GSE162454 dataset. STC2 expression was assessed across major cell types within the OS microenvironment, including Endothelial, Fibroblasts, and Malignant cells. Cell-cell interaction (CCI) analysis was performed to examine potential interactions between Endothelial cells and other cell populations with relatively high STC2 expression. In addition, Gene Set Enrichment Analysis (GSEA) was conducted to compare enriched biological pathways between high- and low-STC2 expression groups.

Pan-cancer analysis of STC2 expression and its prognostic implications

We conducted a comprehensive pan-cancer analysis of STC2 expression using the TCGA database to evaluate its role across multiple cancer types. Differential expression of STC2 was assessed between tumor and normal tissues across all cancer types, followed by paired tumor-normal sample comparisons to confirm the observed expression patterns. Prognostic significance of STC2 was evaluated using survival data, including Disease-Free Interval (DFI), Disease-Specific Survival (DSS), Overall Survival, and Progression-Free Interval (PFI). The association between STC2 expression and key genomic features, including Tumor Mutational Burden (TMB) and Microsatellite Instability (MSI), was also explored. Additionally, GSEA was performed based on the Hallmark gene set to identify biological pathways enriched in both high and low STC2 expression groups.

Immune infiltration and immunotherapy response prediction based on STC2 expression

To investigate the potential therapeutic impact of STC2 expression in OS, we quantified immune cell infiltration using six well-established algorithms: Cibersort [18], EPIC [19], quanTIseq [20], TIMER [21], MCPCounter [22], and xCell [23]. These algorithms were employed to assess immune cell populations in OS samples, followed by differential expression analysis to compare immune profiles between patients with high and low STC2 expression. Additionally, we analyzed the expression of common immune checkpoint genes, including both inhibitory and stimulatory genes, and performed TIDE (Tumor Immune Dysfunction and Exclusion) and SubMap analyses as computational, exploratory tools to estimate the potential association between STC2 expression groups and predicted response to immune checkpoint blockade [24,25].

Cell culture

Human osteosarcoma cell lines U2OS and 143B were cultured in Dulbecco's Modified Eagle Medium (DMEM) supplemented with 10 % fetal bovine serum (FBS), 100 U/mL penicillin, and 100 μg/mL streptomycin at 37 °C in a humidified incubator with 5 % CO_2.

Lentiviral packaging and cell transduction

Lentiviral particles were generated in HEK293T cells using a three-plasmid system. HEK293T cells were co-transfected with the lentiviral vector, psPAX2, and pMD2.G using Lipofectamine 2000. Viral supernatants were collected at 48 h and 72 h, centrifuged to remove cell debris, and filtered through a 0.45 μm membrane. U2OS and 143B cells were then transduced with lentiviral particles carrying shRNA targeting STC2 or the corresponding negative control for subsequent experiments.

qPCR analysis

Total RNA was extracted using TRIzol reagent according to the manufacturer's instructions. Complementary DNA (cDNA) was synthesized using a reverse transcription kit. Quantitative PCR (qPCR) was performed using SYBR Green PCR Master Mix on a real-time PCR system. Relative expression levels were calculated using the 2^-ΔΔCt method, with GAPDH as the internal control. Each experiment was performed in three independent biological replicates.

Cell proliferation assays

Cell proliferation was evaluated using CCK-8, colony formation, and EdU incorporation assays. For the CCK-8 assay, cells were seeded into 96-well plates at a density of 5000 cells/well. At the indicated time points, CCK-8 reagent was added and absorbance at 450 nm was measured after 2 h of incubation. For the colony formation assay, cells were seeded into 6-well plates at a density of 1000 cells/well and cultured for 10 days, with the medium changed every 3 days. Colonies were then fixed with methanol, stained with 0.1 % crystal violet, and colonies containing >50 cells were counted. For the EdU assay, cells were incubated with EdU for 2 h, followed by fixation, permeabilization, and staining according to the manufacturer's instructions. EdU-positive cells were visualized by fluorescence microscopy and quantified.

Migration and invasion assays

Cell migration assays were performed using transwell chambers without a Matrigel coating, while invasion assays utilized Matrigel-coated chambers. Cells were seeded into the upper chamber in serum-free medium and allowed to migrate or invade towards the lower chamber containing medium supplemented with 10 % FBS. After 24 h, cells on the lower side of the membrane were fixed, stained, and counted.

Results

Impact of calcium homeostasis on OS prognosis and gene expression

Prior to batch correction, the distributions of the Target-OS and GSE42352 datasets showed clear discrepancies, indicating the presence of batch effects (*Fig. 1A*). After ComBat correction, the distributions of the two datasets became more comparable, with improved alignment in means and variances (*Fig. 1B*). ssGSEA analysis revealed variations in calcium homeostasis pathway scores across OS samples, with the expression profiles displayed alongside clinical features (*Fig. 1C*). Differential analysis showed that metastatic OS samples exhibited significantly lower calcium homeostasis pathway scores than non-metastatic samples (*Fig. 1D*), whereas OS samples showed significantly higher pathway scores than normal controls (*Fig. 1E*), suggesting that calcium homeostasis dysregulation in OS may be dynamic and stage-dependent. Using univariate Cox regression as an initial screening step, 28 candidate prognostic genes associated with survival were retained for downstream analysis (*Fig. 1F*). A correlation heatmap of these 28 genes was generated (*Fig. 1G*), and their potential functional interactions were further explored using a protein-protein interaction (PPI) network (*Fig. 1H*).

Prognostic significance of calcium homeostasis-related genes in OS

Our analysis of machine learning model performance showed that the combination of CoxBoost + RSF achieved the highest C-index across all datasets (*Fig. 2A*). Further optimization of the CoxBoost model identified 51 steps as the optimal setting (*Fig. 2B*). Based on this model, 14 genes associated with calcium homeostasis were selected. The importance of these genes in the model was assessed, with STC2 emerging as the most influential gene based on its high importance score (*Fig. 2C*). This result was further supported by RSF analysis, which also ranked STC2 as the most important gene among the 14 selected variables (*Fig. 2D*). Kaplan-Meier survival analysis demonstrated significant differences in survival between the high- and low-risk groups across all datasets (*Fig. 2E*). Additionally, time-dependent ROC analysis at 1, 3, and 5 years demonstrated favorable predictive performance of the riskScore model in the three cohorts (*Fig. 2F*).

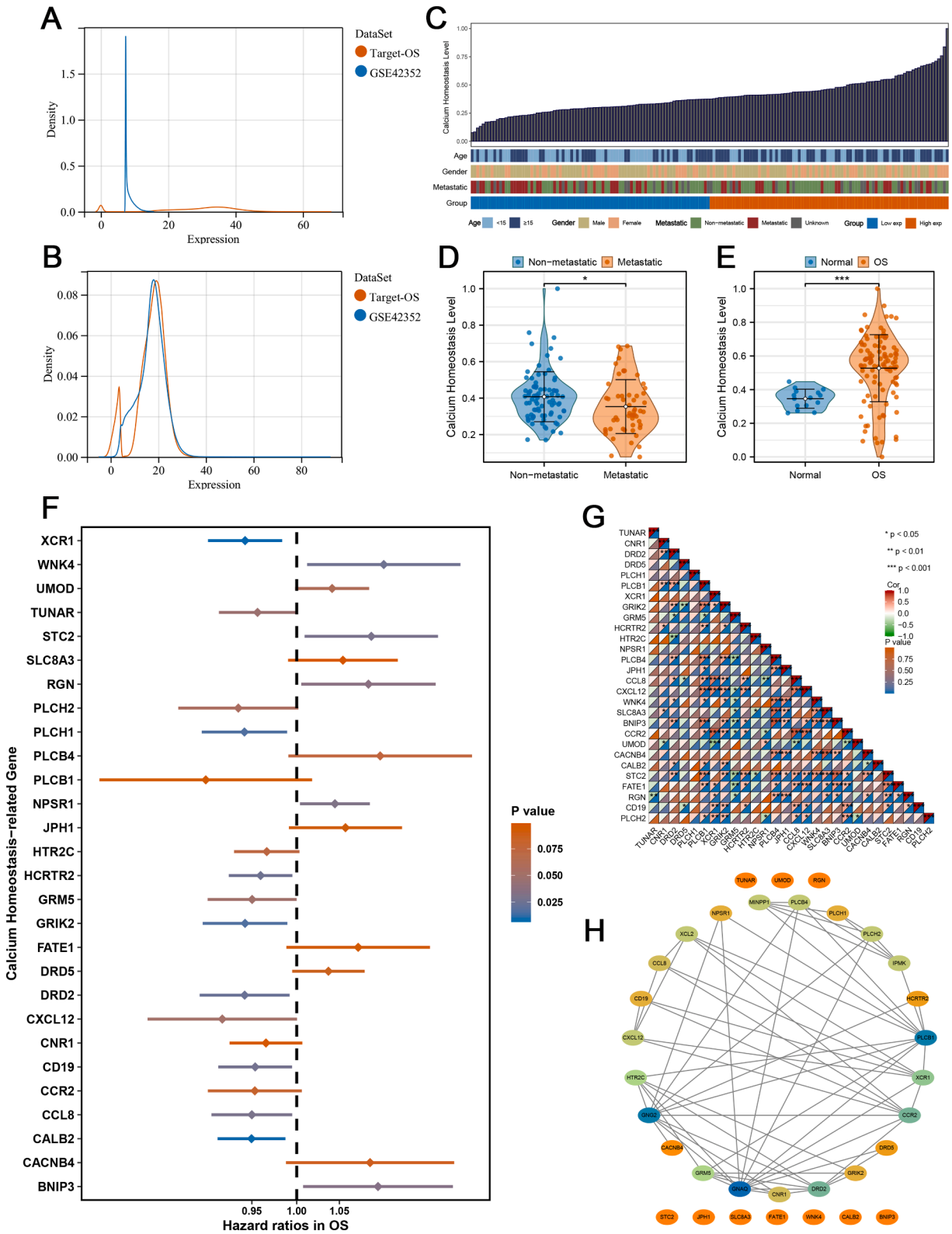

Fig. 1. Analysis of calcium homeostasis pathway expression and prognostic gene identification in OS. (A) Density plots showing the distribution of samples before batch effect correction, indicating significant batch effects between the Target-OS and GSE42352 datasets. (B) Density plots after batch effect correction, demonstrating improved alignment of sample distributions with similar means and variances. (C) ssGSEA quantification of calcium homeostasis pathway expression across OS samples and its relationship with clinical features. (D) Differential expression analysis of calcium homeostasis levels between metastatic and non-metastatic OS patients. (E) Comparison of calcium homeostasis pathway expression levels between OS samples and normal controls. (F) Forest plot showing the 28 prognostic genes significantly associated with OS patient prognosis based on univariate Cox regression analysis. (G) Correlation heatmap illustrating relationships among the 28 prognostic genes identified in univariate Cox regression. (H) Protein-protein interaction (PPI) network depicting the functional interactions among the 28 prognostic genes.

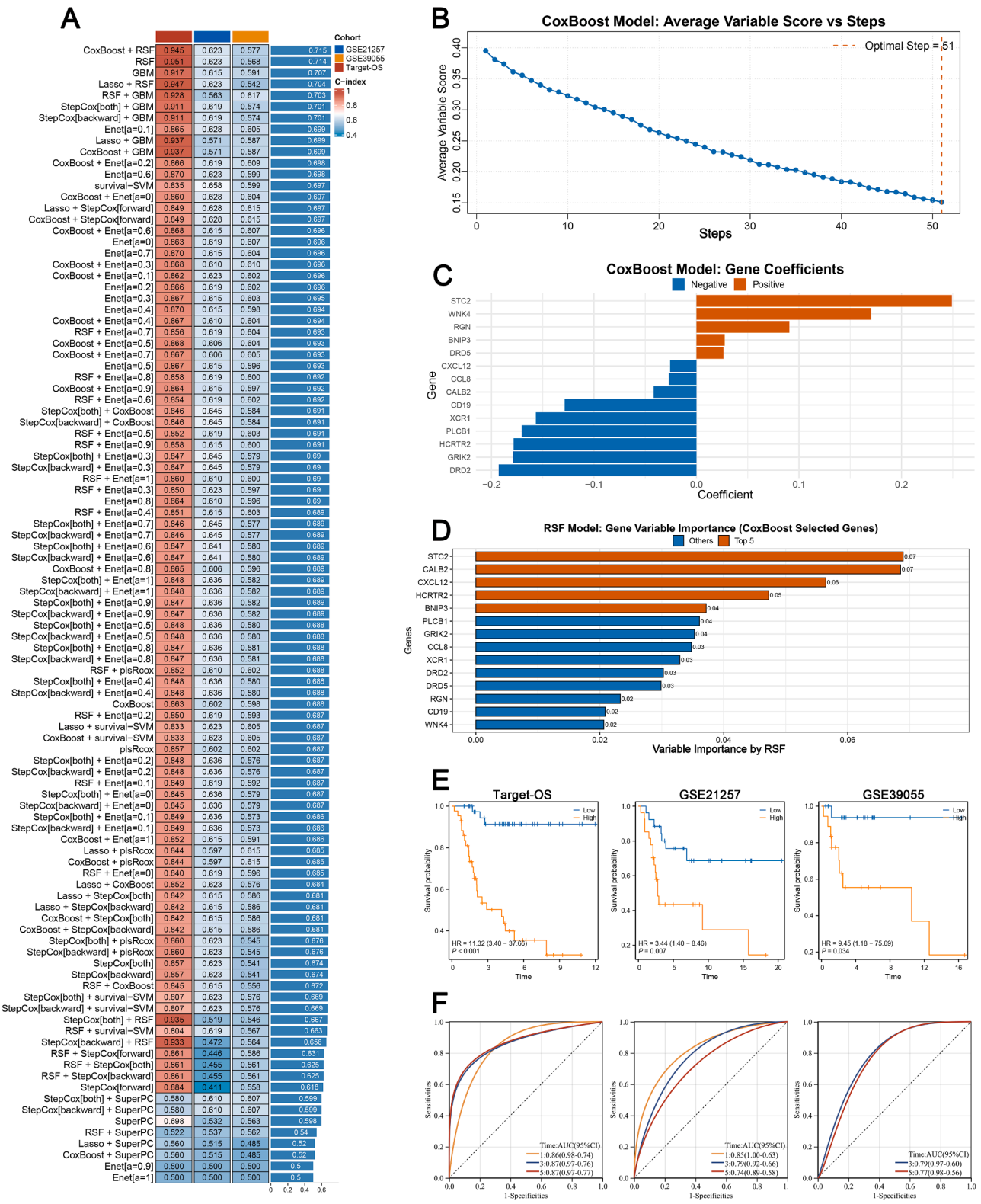

Fig. 2. Performance and validation of prognostic models for calcium homeostasis-related genes in OS. (A) Ranking of machine learning algorithms based on the average C-index across all datasets. The combination of CoxBoost + RSF achieved the highest C-index. (B) Performance of the CoxBoost algorithm, showing that the optimal number of steps for the best model performance is 51. (C) Importance coefficients of the 14 selected genes in the final CoxBoost + RSF model. (D) RSF analysis of the 14 selected genes, with STC2 identified as the most significant gene. (E) Kaplan-Meier survival curves for patients stratified into high- and low-risk groups based on the median riskScore in all three datasets. (F) Time-dependent ROC curves for 1-, 3-, and 5-year survival predictions using the riskScore model.

Prognostic significance of risk score in immune pathways and biological pathways

The correlation analysis showed that riskScore exhibited limited correlations with most immune therapy–related pathways and Hallmark pathways. However, relatively stronger associations were observed with the glycolysis and unfolded protein response (UPR) pathways (*Fig. 3A*). Subsequently, GO enrichment analysis revealed distinct biological processes associated with the high- and low-risk groups. In the high-risk group, the most enriched biological processes included detection of chemical stimulus involved in sensory perception and translation regulator activity (*Fig. 3B*). In contrast, the low-risk group showed significant enrichment in pathways related to the T cell receptor complex and immunoglobulin complex (*Fig. 3C*). KEGG pathway analysis further identified the NOD-like receptor signaling pathway as significantly enriched in the high-risk group, while the ribosome pathway was enriched in the low-risk group (*Fig. 3D, E*).

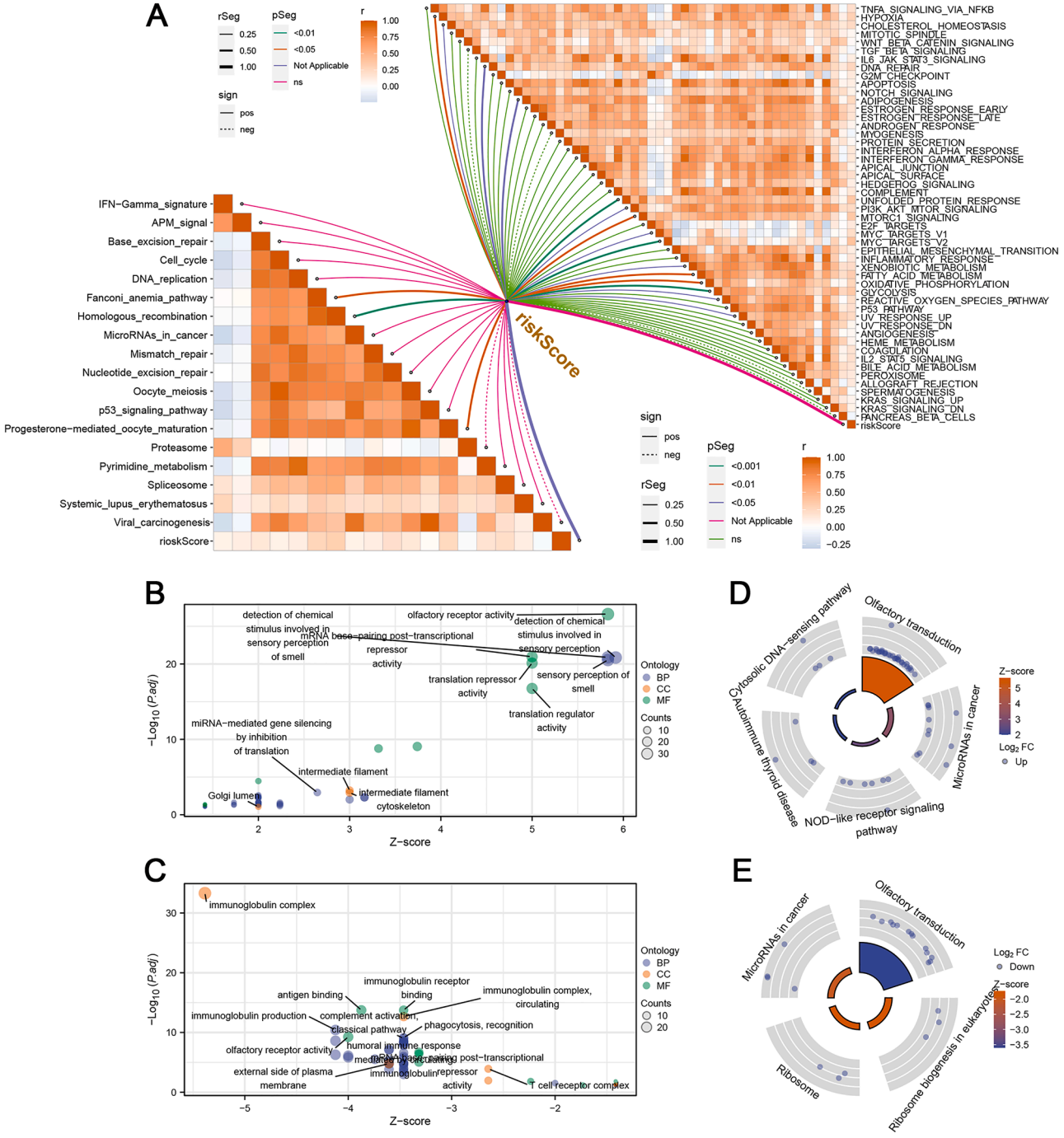

Fig. 3. Relationship between risk score and biological pathways: immune, GO, and KEGG analyses. (A) correlation between riskscore and immune therapy-related pathways, as well as hallmark pathways. (B) GO enrichment analysis for the high-risk group, highlighting biological processes such as detection of chemical stimulus involved in sensory perception and translation regulator activity. (C) GO enrichment analysis for the low-risk group, identifying pathways related to the T cell receptor complex and immunoglobulin complex. (D) KEGG analysis for the high-risk group, showing significant enrichment in the NOD-like receptor signaling pathway. (E) KEGG analysis for the low-risk group, demonstrating enrichment of the ribosome pathway.

STC2 expression and its correlation with cellular profiles and pathways

Our analysis revealed that STC2 was highly expressed in Endothelial, Fibroblasts, and Malignant cell types, with the Endothelial cluster showing the highest expression levels (*Fig. 4A, B*). CCI analysis highlighted significant interactions between Endothelial cells and other cell types within the OS microenvironment (*Fig. 4C*). GSEA of high- and low-expression groups of STC2 identified distinct enrichment patterns in biological pathways, with the high-expression group showing specific pathway associations, while the low-expression group exhibited a different set of enriched pathways (*Fig. 4D, E*).

Immune landscape and immunotherapy response based on STC2 expression

We observed significant differences in immune cell infiltration between high and low STC2 expression groups, with macrophage infiltration showing consistent variations across all six algorithms (*Fig. 5A*). Differential expression analysis revealed marked differences in the levels of inhibitory immune checkpoint genes (*Fig. 5B*) and stimulatory

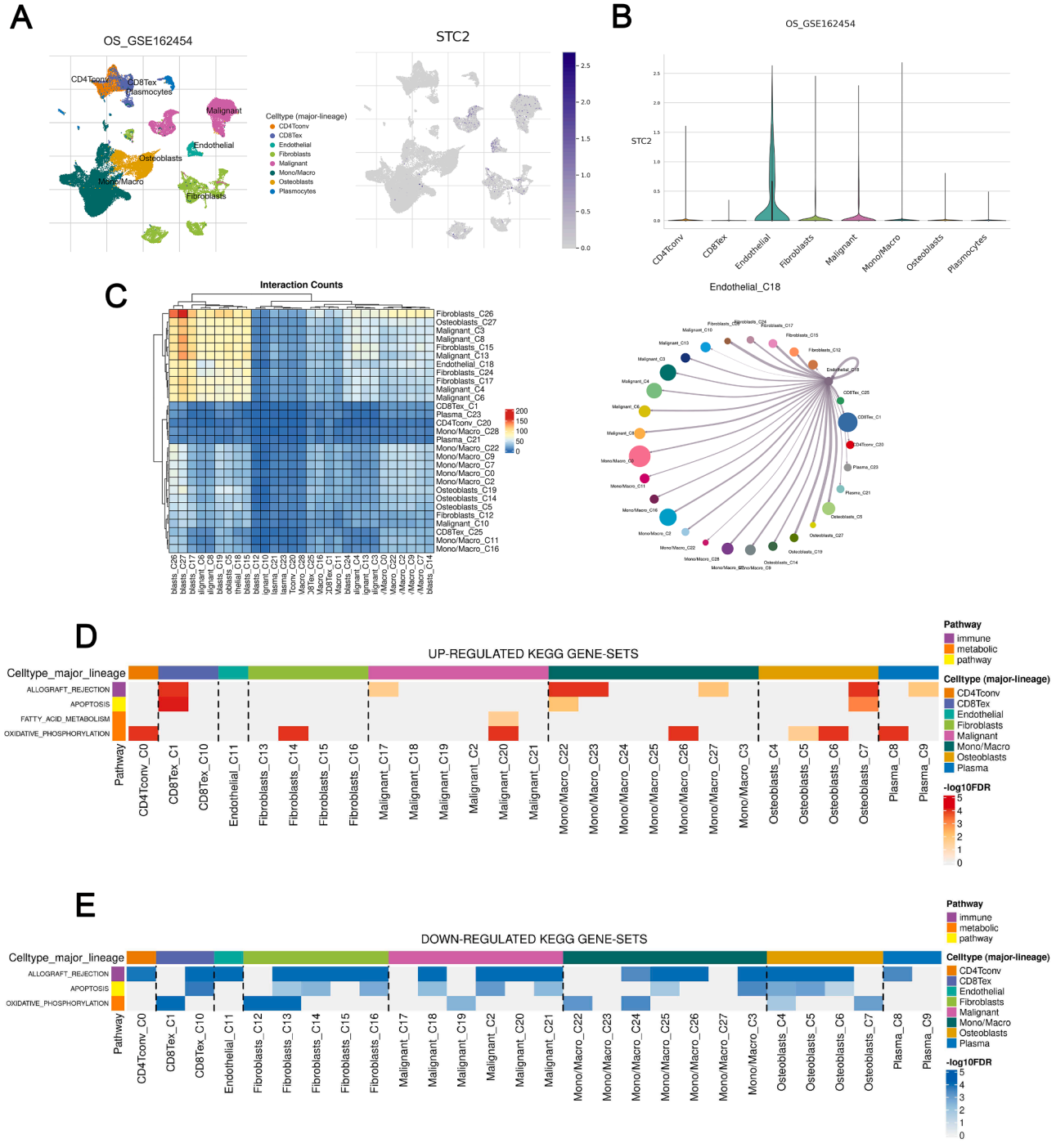

Fig. 4. Single-cell and pathway analysis of STC2 in OS. (A) Expression levels of STC2 across various cell types in the OS_GSE162454 dataset. (B) Visual depiction of STC2 expression across different cell clusters, highlighting the endothelial cluster as the predominant source of expression. (C) CCI analysis showing interactions between Endothelial cells and other cell populations in the OS microenvironment. (D) GSEA of high- and low-expression groups of STC2, revealing distinct enrichment patterns in biological pathways.

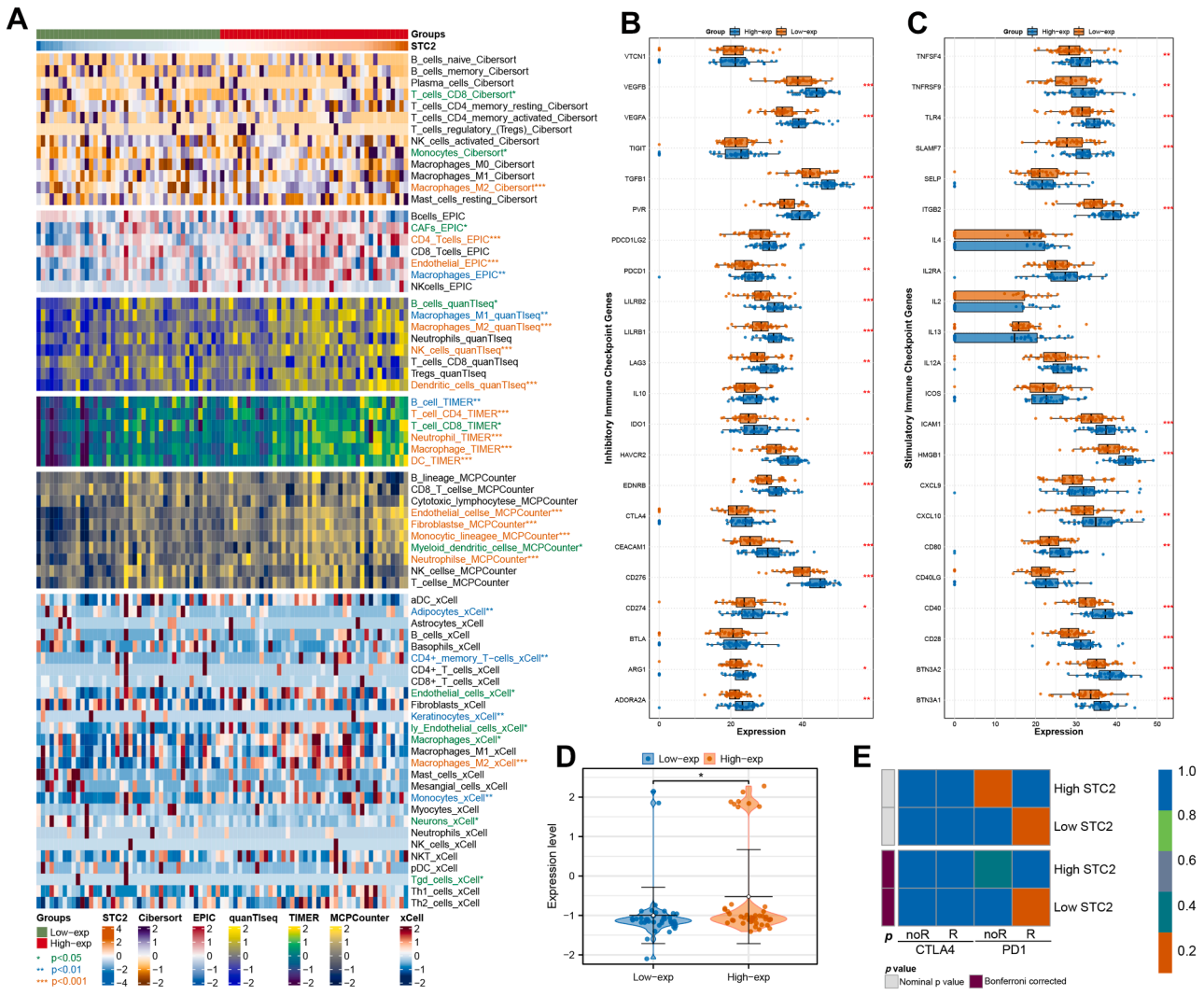

Fig. 5. Immune infiltration and immunotherapy response in OS based on STC2 Expression. (A) Differences in immune cell infiltration between high and low STC2 expression groups, assessed using six immune infiltration algorithms. (B-C) Differential expression of inhibitory and stimulatory immune checkpoint genes between high and low STC2 expression groups. (D) TIDE analysis showing significantly lower TIDE scores in the low STC2 expression group, indicating a higher potential for immune therapy response. (E) Submap analysis suggesting that low STC2 expression is associated with a better response to immune checkpoint inhibitors.

immune checkpoint genes (*Fig. 5C*) between the two groups. Notably, TIDE analysis showed that patients with low STC2 expression exhibited significantly lower TIDE scores, suggesting a computationally predicted higher likelihood of response to immune checkpoint inhibitors (*Fig. 5D*). Consistently, SubMap analysis also supported a potential association between low STC2 expression and a more favorable predicted response to immunotherapy (*Fig. 5E*). However, these findings should be interpreted as in silico predictions rather than clinically validated treatment outcomes.

Expression and prognostic value of STC2 across cancer types

Pan-cancer analysis revealed that STC2 was overexpressed in most cancer types compared to normal tissues (*Fig. 6A*). Paired tumor-normal differential expression analysis confirmed this finding (*Fig. 6B*). Prognostic analysis showed that STC2 has varying prognostic roles depending on the cancer type and survival endpoint (DFI, DSS, OS, PFI) (*Fig. 6C*). Forest plot analysis for overall survival data indicated that STC2 is a risk factor in several cancers, including sarcoma (SARC) (*Fig. 6D*). Moreover, STC2 expression was positively correlated with both TMB and MSI in SARC (*Fig. 6E, F*). Finally, GSEA based on the Hallmark gene set revealed significant pathway enrichments in high and low STC2 expression groups across different cancer types (*Fig. 6G*).

Knockdown of STC2 hampers the proliferation, invasion and migration ability of OS cells

We first examined STC2 expression in osteosarcoma (OS) cell lines. qPCR analysis showed that STC2 expression was significantly higher in OS cells than in hFOB cells (*Fig. 7A*). To further investigate the biological functions of STC2, we selected U2OS and 143B cell lines for subsequent experiments. STC2-knockdown cells were established, and the knockdown efficiency was confirmed by qPCR (*Fig. 7B-C*). Among the tested shRNAs, sh-STC2#2 showed the highest knockdown efficiency and was therefore used in the downstream experiments. CCK-8 and colony formation assays showed that STC2 knockdown significantly suppressed the proliferative capacity of OS cells (*Fig. 7D-F*). Consistently, EdU assays showed a consistent trend, with a marked reduction in DNA synthesis following STC2 knockdown (*Fig. 7G*). Furthermore, Transwell assays indicated a significant decrease in both the invasive and migratory abilities of OS cells upon STC2 knockdown (*Fig. 8A-B*). Together, these results suggest that STC2 is highly expressed in OS cells and may play a pro-tumorigenic role by promoting cell proliferation, invasion, and migration.

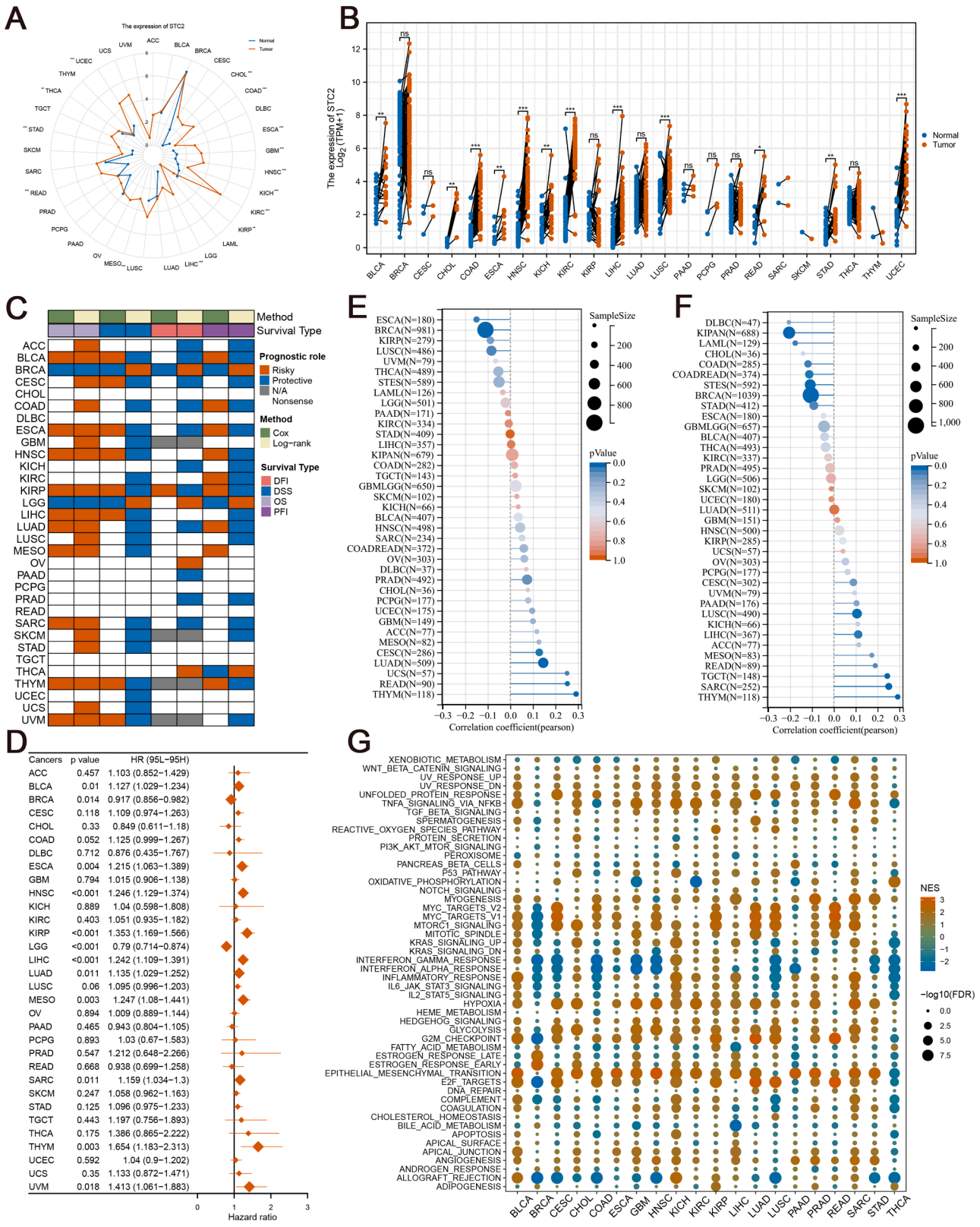

Fig. 6. Pan-cancer profiling of STC2 expression and its prognostic implications. (A) Differential expression of STC2 between tumor and normal tissues across various cancer types in the TCGA database. (B) Paired tumor-normal differential expression analysis confirming consistent overexpression of STC2 in multiple cancers. (C) Prognostic significance of STC2 across cancer types, assessed using multiple survival endpoints (DFI, DSS, OS, PFI). (D) Forest plot illustrating the prognostic value of STC2 in OS, identifying it as a risk factor in multiple cancers, including SARC. (E-F) Correlation analysis between STC2 expression and tumor mutational burden (TMB) and microsatellite instability (MSI). (G) GSEA based on the Hallmark gene set, comparing high and low STC2 expression groups.

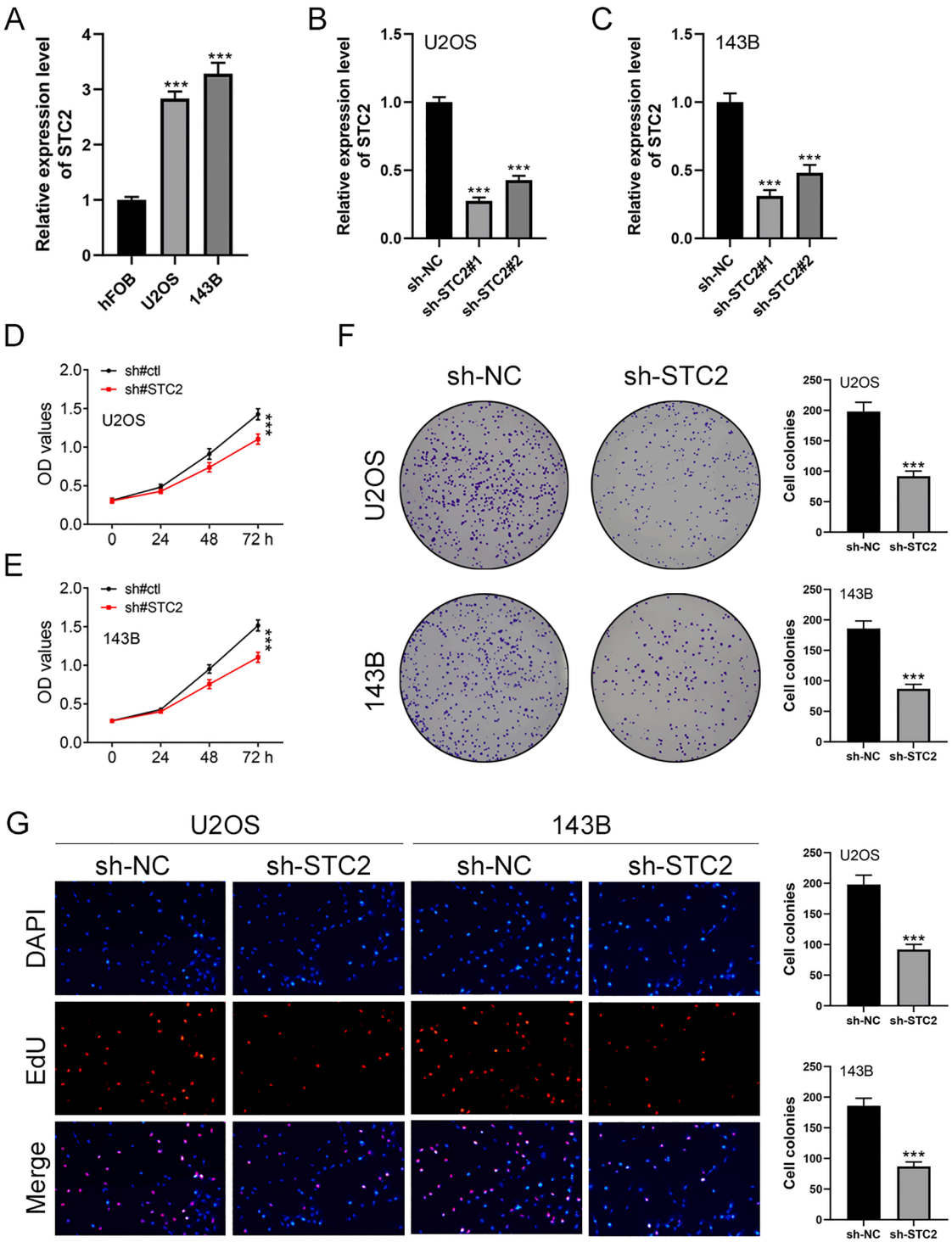

Fig. 7. STC2 is highly expressed in OS cells and promotes cell proliferation. (A) qPCR analysis showing the expression levels of STC2 in OS cell lines compared to normal cells. (B-C) Validation of STC2 knockdown efficiency in U2OS and 143B cells using qPCR. (D-F) CCK-8 and colony formation assays showing decreased proliferation capacity in STC2-knockdown OS cells. (G) EdU assay demonstrating reduced DNA synthesis in STC2-knockdown OS cells.

Discussion

In this study, we utilized a comprehensive machine learning approach to explore the role of calcium homeostasis-related genes in the prognosis of OS. Our findings underscore the pivotal role of calcium homeostasis, particularly STC2, as a prognostic biomarker and potential therapeutic target in OS. By integrating transcriptomic data and clinical outcomes, we identified key genes involved in calcium regulation that can effectively predict patient survival. Moreover, our study highlights the potential for incorporating immune landscape profiling into OS prognosis models, which could pave the way for personalized immunotherapeutic strategies.

Our results demonstrate that metastatic OS patients exhibit significantly lower expression of calcium homeostasis genes compared to their non-metastatic counterparts, suggesting a potential role for calcium signaling in OS metastasis. This finding is in line with existing studies

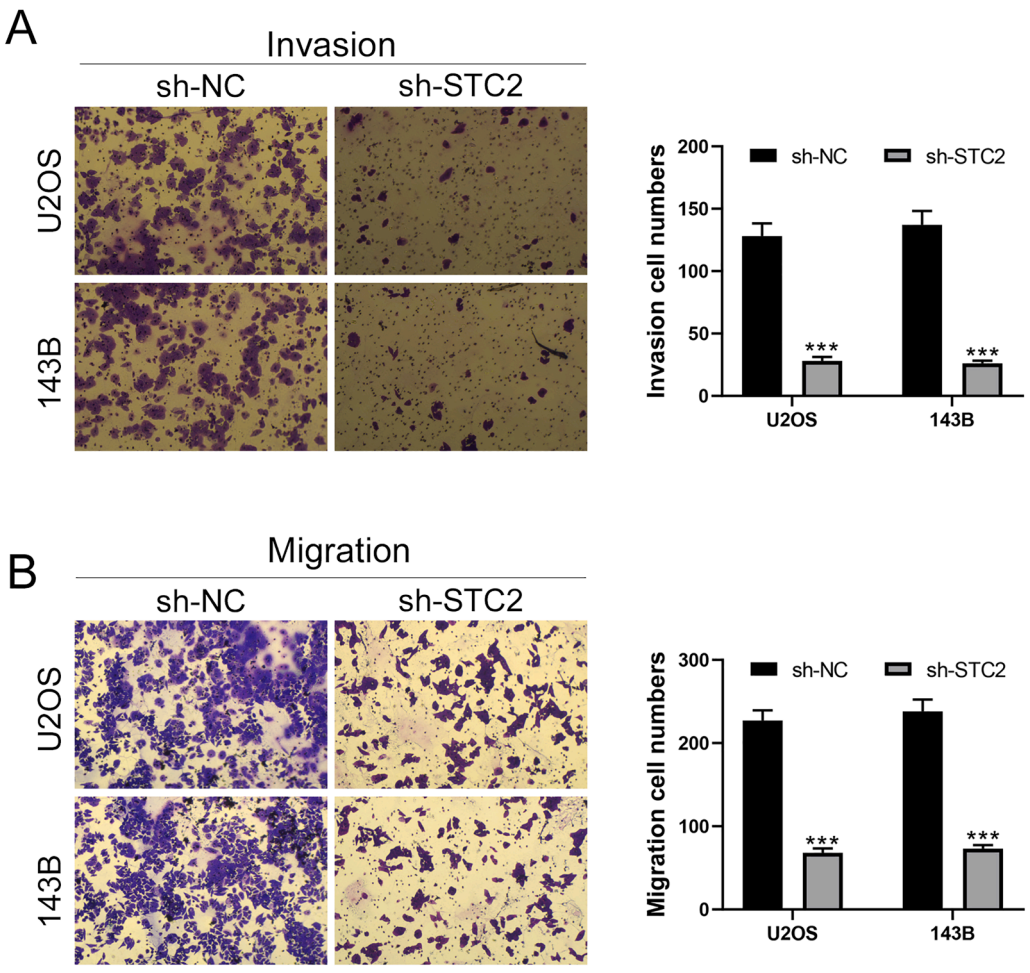

Fig. 8. STC2 promotes OS cell invasion and migration. (A-B) Transwell assays showing reduced invasion and migration abilities in STC2-knockdown OS cells.

indicating that altered calcium signaling can facilitate processes such as epithelial-mesenchymal transition (EMT), which plays a critical role in the metastatic spread of cancer [26,27]. However, the precise molecular mechanisms linking calcium dysregulation to OS metastasis remain an area for further exploration. In our experimental validation, we observed that STC2 was significantly overexpressed in OS cell lines compared to normal cells, and STC2 knockdown in U2OS and 143B cells inhibited cell proliferation, migration, and invasion, supporting the idea that STC2 may contribute to metastatic progression in OS.

The identification of STC2 as a critical prognostic gene is a significant finding in this study. Our machine learning models, particularly CoxBoost and RSF, highlighted STC2 as the most important gene for survival prediction in OS patients. The robust performance of these models was validated by Kaplan-Meier survival analysis. This suggests that STC2 could serve as a reliable biomarker for risk stratification in OS, potentially guiding clinical decision-making for more personalized treatment approaches. Experimental assays, including CCK-8, colony formation assays, and EdU incorporation assays, confirmed that STC2 knockdown significantly reduced the proliferation capacity of OS cells, aligning with the machine learning results and reinforcing the role of STC2 in OS progression.

Furthermore, the single-cell expression profiling in our study revealed that STC2 is predominantly expressed in endothelial, fibroblast, and malignant cells, with the highest expression observed in endothelial cells. This finding suggests that STC2 may exert its effects not only within cancer cells but also through interactions with the tumor microenvironment, particularly endothelial cells, which play a critical role in angiogenesis and metastasis [28,29]. The observed cell-cell interactions provide valuable insights into how STC2 may influence OS progression and immune modulation.

A key aspect of this study was the exploration of STC2 expression in relation to immune infiltration and response to immunotherapy. Our analysis revealed significant differences in immune cell profiles between high and low STC2 expression groups, particularly in the infiltration of macrophages, which are known to influence tumor progression and the immune response [30,31]. In addition, differential expression analysis of immune checkpoint genes indicated that STC2 expression correlates with the modulation of both inhibitory and stimulatory immune checkpoints.

In addition, TIDE and SubMap analyses suggested that patients with low STC2 expression may have a more favorable predicted response to immune checkpoint blockade. However, these results were derived from computational algorithms rather than from an osteosarcoma cohort treated with immunotherapy, and therefore should be interpreted as exploratory and hypothesis-generating rather than clinically validated evidence. Although TIDE and SubMap are widely used for immunotherapy response prediction and have also been applied in osteosarcoma-related bioinformatic studies [32], further validation in independent immunotherapy-treated osteosarcoma cohorts will be necessary before STC2 can be considered an established predictive biomarker.

Although our study provides valuable insights into the role of STC2 in OS, several limitations must be considered. First, the data were derived from publicly available datasets, which may not fully represent the molecular heterogeneity of OS across different patient populations. Larger, multi-center, prospective studies are needed to validate our

findings. Second, while machine learning models showed promising results, their predictive accuracy could be improved by incorporating additional molecular data. Third, functional validation of STC2 was limited to in vitro knockdown assays; rescue experiments and in vivo studies were not performed, and the direct mechanistic link to calcium homeostasis and immune modulation remains untested. Finally, predictions regarding immunotherapy response were based on computational algorithms (TIDE and SubMap) rather than clinical data from OS patients treated with immune checkpoint inhibitors, and therefore should be interpreted cautiously as hypothesis-generating.

Declaration of generative AI use

The authors did not use generative AI or AI-assisted technologies in the preparation of this manuscript.

Ethics approval

Not applicable.

CRediT authorship contribution statement

Kang Yao: Visualization, Software, Resources, Methodology, Investigation, Formal analysis, Data curation, Conceptualization. **Qian Jiawei:** Visualization, Software, Methodology, Investigation, Formal analysis, Data curation, Conceptualization. **Xu Jietao:** Validation, Supervision, Data curation. **Wang Xijun:** Methodology, Investigation, Formal analysis. **Zhou Hong:** Visualization, Validation, Software. **Bi Qing:** Writing – review & editing, Writing – original draft, Supervision, Project administration, Funding acquisition. **Lv Jun:** Writing – review & editing, Writing – original draft, Supervision, Project administration, Funding acquisition.

Declaration of competing interest

The authors declared no competing interests.

Acknowledgements

Not applicable.

Funding: This research was supported by grants from Zhejiang Provincial Natural Science Foundation of China under Grant No LQ24H160045 and Zhejiang Provincial Health Bureau Science Foundation of China, NO. 2024KY647 Found.

Data availability

All datasets used in this study are described in detail in the Methods section. Additional information and materials supporting the findings of this work are available from the corresponding author upon reasonable request.

References

[1] J. Ritter, S.S. Bielack, Osteosarcoma, Ann. Oncol. 21 (7) (2010). Supplvii320-5.
[2] M. Kansara, M.W. Teng, M.J. Smyth, D.M. Thomas, Translational biology of osteosarcoma, Nat. Rev. Cancer 14 (11) (2014) 722–735.
[3] D. Ebb, P. Meyers, H. Grier, M. Bernstein, R. Gorlick, S.E. Lipshultz, et al., Phase II trial of trastuzumab in combination with cytotoxic chemotherapy for treatment of metastatic osteosarcoma with human epidermal growth factor receptor 2 overexpression: a report from the children's oncology group, J. Clin. Oncol. 30 (20) (2012) 2545–2551.
[4] Z. Dai, Y. Sun, M. Maihemuti, R. Jiang, Genome-wide identification of alternative splicing and splicing regulated in immune infiltration in osteosarcoma patients, Front. Genet. 14 (2023) 1051192.
[5] T.Y.S. Le Large, M.F. Bijlsma, G. Kazemier, H.W.M. van Laarhoven, E. Giovannetti, C.R Jimenez, Key biological processes driving metastatic spread of pancreatic cancer as identified by multi-omics studies, Semin. Cancer Biol. 44 (2017) 153–169.
[6] K.J. Alzayady, A. Sebé-Pedrós, R. Chandrasekhar, L. Wang, I. Ruiz-Trillo, D.I. Yule, Tracing the evolutionary history of inositol, 1, 4, 5-trisphosphate receptor: insights from analyses of capsaspora owczarzaki Ca2+ release channel orthologs, Mol. Biol. Evol. 32 (9) (2015) 2236–2253.
[7] S. Zheng, X. Wang, D. Zhao, H. Liu, Y. Hu, Calcium homeostasis and cancer: insights from endoplasmic reticulum-centered organelle communications, Trends. Cell Biol. 33 (4) (2023) 312–323.
[8] A.M. Barradas, H.A. Fernandes, N. Groen, Y.C. Chai, J. Schrooten, J. van de Peppel, et al., A calcium-induced signaling cascade leading to osteogenic differentiation of human bone marrow-derived mesenchymal stromal cells, Biomaterials 33 (11) (2012) 3205–3215.
[9] M. Peterlik, E. Kállay, H.S. Cross, Calcium nutrition and extracellular calcium sensing: relevance for the pathogenesis of osteoporosis, cancer and cardiovascular diseases, Nutrients 5 (1) (2013) 302–327.
[10] E. Izquierdo-Torres, A. Hernández-Oliveras, G. Fuentes-García, Á. Zarain-Herzberg, Calcium signaling and epigenetics: a key point to understand carcinogenesis, Cell Calcium. 91 (2020) 102285.
[11] J. Goecks, V. Jalili, L.M. Heiser, J.W. Gray, How machine learning will transform biomedicine, Cell 181 (1) (2020) 92–101.
[12] N. Zhang, H. Zhang, W. Wu, R. Zhou, S. Li, Z. Wang, et al., Machine learning-based identification of tumor-infiltrating immune cell-associated lncRNAs for improving outcomes and immunotherapy responses in patients with low-grade glioma, Theranostics 12 (13) (2022) 5931–5948.
[13] J. Liu, Y. Shi, Y. Zhang, Multi-omics identification of an immunogenic cell death-related signature for clear cell renal cell carcinoma in the context of 3P medicine and based on a 101-combination machine learning computational framework, EPMa J. 14 (2) (2023) 275–305.
[14] D. Zhang, K. Zhao, T. Han, X. Zhang, X. Xu, Z. Liu, et al., Bisphenol A promote the cell proliferation and invasion ability of prostate cancer cells via regulating the androgen receptor, Ecotoxicol. Environ. Saf. 269 (2024) 115818.
[15] J. Taminau, S. Meganck, C. Lazar, D. Steenhoff, A. Coletta, C. Molter, et al., Unlocking the potential of publicly available microarray data using inSilicoDb and inSilicoMerging R/bioconductor packages, BMC. Bioinf. 13 (2012) 335.
[16] W.E. Johnson, C. Li, A. Rabinovic, Adjusting batch effects in microarray expression data using empirical Bayes methods, Biostatistics 8 (1) (2007) 118–127.
[17] J. Hu, A. Yu, B. Othmane, D. Qiu, H. Li, C. Li, et al., Siglec15 shapes a non-inflamed tumor microenvironment and predicts the molecular subtype in bladder cancer, Theranostics 11 (7) (2021) 3089–3108.
[18] A.M. Newman, C.L. Liu, M.R. Green, A.J. Gentles, W. Feng, Y. Xu, et al., Robust enumeration of cell subsets from tissue expression profiles, Nat. Methods 12 (5) (2015) 453–457.
[19] J. Racle, K. de Jonge, P. Baumgaertner, D.E. Speiser, D. Gfeller, Simultaneous enumeration of cancer and immune cell types from bulk tumor gene expression data, Elife 6 (2017).
[20] F. Finotello, C. Mayer, C. Plattner, G. Laschober, D. Rieder, H. Hackl, et al., Correction to: molecular and pharmacological modulators of the tumor immune contexture revealed by deconvolution of RNA-seq data, Genome Med. 11 (1) (2019) 50.
[21] B. Li, E. Severson, J.C. Pignon, H. Zhao, T. Li, J. Novak, et al., Comprehensive analyses of tumor immunity: implications for cancer immunotherapy, Genome Biol. 17 (1) (2016) 174.
[22] E. Becht, N.A. Giraldo, L. Lacroix, B. Buttard, N. Elarouci, F. Petitprez, et al., Erratum to: estimating the population abundance of tissue-infiltrating immune and stromal cell populations using gene expression, Genome Biol. 17 (1) (2016) 249.
[23] D. Aran, Z. Hu, A.J. Butte, XCell: digitally portraying the tissue cellular heterogeneity landscape, Genome Biol. 18 (1) (2017) 220.
[24] P. Jiang, S. Gu, D. Pan, J. Fu, A. Sahu, X. Hu, et al., Signatures of T cell dysfunction and exclusion predict cancer immunotherapy response, Nat. Med. 24 (10) (2018) 1550–1558.
[25] Y. Hoshida, J.P. Brunet, P. Tamayo, T.R. Golub, J.P. Mesirov, Subclass mapping: identifying common subtypes in independent disease data sets, PLoS. One 2 (11) (2007) e1195.
[26] I. Ota, T. Masui, M. Kurihara, J.I. Yook, S. Mikami, T. Kimura, et al., Snail-induced EMT promotes cancer stem cell-like properties in head and neck cancer cells, Oncol. Rep. 35 (1) (2016) 261–266.
[27] M. Liaghat, S. Ferdousmakan, S.H. Mortazavi, S. Yahyazadeh, A. Irani, S. Banihashemi, et al., The impact of epithelial-mesenchymal transition (EMT) induced by metabolic processes and intracellular signaling pathways on chemo-resistance, metastasis, and recurrence in solid tumors, Cell Commun. Signal. 22 (1) (2024) 575.
[28] T. Watabe, K. Takahashi, K. Pietras, Y. Yoshimatsu, Roles of TGF-β signals in tumor microenvironment via regulation of the formation and plasticity of vascular system, Semin. Cancer Biol. 92 (2023) 130–138.
[29] J.W. Franses, N.C. Drosu, W.J. Gibson, V.C. Chitalia, E.R. Edelman, Dysfunctional endothelial cells directly stimulate cancer inflammation and metastasis, Int. J. Cancer 133 (6) (2013) 1334–1344.
[30] C.E. Lewis, A.S. Harney, J.W. Pollard, The multifaceted role of perivascular macrophages in tumors, Cancer Cell. 30 (1) (2016) 18–25.
[31] L. Yang, Y. Zhang, Tumor-associated macrophages: from basic research to clinical application, J. Hematol. Oncol. 10 (1) (2017) 58.
[32] Y. Wang, X. Wang, Y. Liu, J. Xu, J. Zhu, Y. Zheng, et al., A novel hypoxia- and lactate metabolism-related prognostic signature to characterize the immune landscape and predict immunotherapy response in osteosarcoma, Front. Immunol. 15 (2024) 1467052.